Measurements of the electron-impact double-to-single ionization ratio using trapped lithium

M.-T. Huang, L. Zhang, S. Hasegawa,* S. H. Southworth, and L. Young
Argonne National Laboratory, 9700 South Cass Avenue, Argonne, Illinois 60439
(Received 10 April 2002; published 25 July 2002)

The Li^{2+} to Li^{+} production cross-section ratio of ground-state atomic Li by electron-impact ionization has been measured for electron energies ranging from 200 eV to 1500 eV. The measurements were done using a pulsed, ion imaging time-of-flight spectrometer with Li atoms confined in a magneto-optical trap. The ratios are more accurate than the single earlier result for the Li^{2+} to Li^{+} ratios, a composite of two absolute measurements, and are systematically lower. Both experiments show similar energy dependences that disagree with the trend predicted by a semiempirical formulation. These measurements provide a benchmark for theoretical studies of electron-impact double ionization.

DOI: 10.1103/PhysRevA.66.012715 PACS number(s): 32.80.Fb, 32.80.Hd

I. INTRODUCTION

Electron-impact ionization is a fundamental collision process in atomic physics. Because of importance from both applied and theoretical viewpoints, it has been the subject of study for many years [1]. Nevertheless, the predictive power of theory remains limited. Theoretical challenges are great, as even the simplest process, electron-impact single ionization, yields a final state with three charged particles in the continuum. Over the past decade, considerable theoretical progress has been made on electron-impact single ionization based on nonperturbative methods, where calculations in the electron-hydrogen system [2–6] reproduce the observed ionization cross sections to within experimental error bars ($\approx 3\%$) [7] over a wide energy range. For atoms more complex than hydrogen, the agreement between theory and experiment for total ionization cross sections is somewhat less impressive, particularly when target electrons occupy more than one shell, e.g., metastable He $1s2s\ \ ^3S$ and the alkalis [8].

For electron-impact double ionization, an *ab initio* theoretical understanding has started to emerge with sophisticated methods being developed to treat the strongly correlated four-body continuum [9–12]. The theoretical developments have been largely stimulated by $(e,3e)$ experiments in He, where the final state constitutes a pure four-body problem [13–16]. The theoretical focus has been on the observed angular correlation patterns of the two ejected electrons, with less attention paid to the absolute value of the double-ionization cross section. Despite the existence of rather reliable values for the electron-impact double-ionization cross section in helium [17,18] and even more reliable ratios of the double-to-single ionization cross sections, to our knowledge, only one *ab initio*, fully quantal work has calculated this ratio [12]. In that work the authors obtained a value for the double-to-single ionization cross-section ratio for He, which is in reasonable agreement with the experimental observation. For more complex atoms, only semiempirical and semiclassical approaches have been used to predict multiple-ionization cross sections [1,19,20]. The semiempirical approach had qualitative success in reproducing trends and peak values for double-ionization cross sections, but tends to overestimate for metals and underestimate for rare gases by factors of roughly 2 [19].

In this work, we study electron-impact double and single ionization of lithium, an atom that represents the next step in complexity beyond helium. For theoreticians, lithium provides a reasonable computational challenge that can be treated from first principles using some of the new methods developed for electron-impact ionization of hydrogen, e.g., convergent close coupling and time-dependent close coupling [21,22]. Other theoretical studies have used distorted-wave methods to predict ionization cross sections, which are dominated by the single-ionization channel [23–25]. Experimentally, there have been three previous measurements of electron-impact ionization in lithium [26–28], of which only one dealt with the double-ionization channel explicitly [28]. In that study, absolute cross sections were measured for both single- and double-ionization channels by crossing an electron beam with an atomic beam of lithium and using a mass spectrometer to detect the lithium ions. Both channels were measured independently, using different detectors. The well-known difficulties with absolute cross-section measurements, e.g., determining beam intensities, beam impurities, beam overlap, and collection efficiencies, are therefore present for both measurements, and the ratio is not necessarily more accurate than the individual measurement.

In this work, we use lithium atoms confined in a magneto-optical trap (MOT), as a target to study electron-impact ionization by ion time-of-flight (TOF) spectrometry. This eliminates many of the uncertainties present in crossed-beam experiments. Since a MOT confines only specific atoms, the uncertainty due to the presence of dimers or other impurities in the target is eliminated. Moreover, in traditional methods, ions are produced over a relatively large volume, leading to uncertainty from possible differences in collection efficiency for different charge states. This uncertainty is reduced using a MOT since Li ions are produced in a localized spot near the center of the spectrometer and are efficiently extracted to the detector. Using the same detector for all charge states eliminates the problem of cross calibration of detectors present in the earlier lithium measurements. In addition, a

*Permanent address: Department of Quantum Engineering and Systems Science, The University of Tokyo, Tokyo 113-8656, Japan.

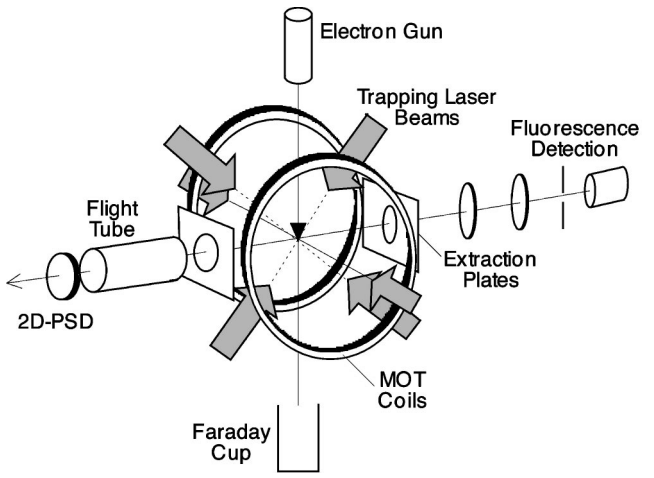

FIG. 1. Schematic of the experimental apparatus (not to scale). See text for details.

MOT can be used to measure absolute electron-impact ionization cross sections using the trap loss method [29] that eliminates the need for absolute density, detection efficiency, and beam intensity measurements. The measured ratio can then be combined with those measurements to obtain the absolute single- and double-ionization cross sections. In addition, a MOT with its low temperature ($\leqslant 1$ mK) and hence low-momentum spread, is a perfect target for recoil ion momentum measurements that can provide insight and visualization of complex ionization processes [30]. Although we do not perform momentum-resolved measurements in this work, we do use the properties of a cold, localized MOT target to project the ions onto a localized spot on a position-sensitive detector and greatly improve the achievable signal to background using position cuts. Our results for the Li^{2+} to Li^{+} ratio by electron impact have an accuracy of $\approx 5\%$ over the 200–1500 eV range, representing a significant improvement over the early results of Jalin *et al.* [28]. Comparison is made with semiempirical calculations [19].

II. EXPERIMENTAL SETUP

The basic experiment is to prepare a sample of ultracold Li atoms at the center of a time-of-flight ion spectrometer. A pulse of electrons is then used to ionize the Li atoms. The resulting ions are extracted onto an imaging detector, with m/q identification being done by the time of flight.

The experimental setup is schematically shown in Fig. 1. A resistively heated oven with a 1-mm orifice was used to produce Li vapor for trapping and was operated typically at $\approx 320\,^{\circ}$C. The oven was located ≈ 10 cm from the trapping region in a differentially pumped source chamber. The Li vapor entered the trapping chamber through a 4-mm aperture. A shutter located between this aperture and the oven orifice was used to admit Li vapor to the experimental chamber during the MOT loading period and to block the Li beam during the ionization measurements. The background pressure was maintained at about 2×10^{-9} Torr during the experiment. The magnetic-field gradient of 8 G/cm was produced by water-cooled, anti-Helmholtz coils located inside the chamber. The low-inductance coils (≈ 4 μH) permitted rapid turnoff (≈ 50 μs) of the magnetic field; the absence of the magnetic field is necessary to control the low-energy electron-beam trajectories.

The trapping laser light was provided by a ring laser operating with DCM dye. A small fraction of the beam was split and used for diagnostics and frequency locking. Using the diagnostic beam, the central frequency of the laser was shifted by 100 MHz using an acousto-optic modulator (AOM) and then locked to the $2\,^2S_{1/2}$ ($F=3/2$) to $2\,^2P_{3/2}$ ($F'=5/2$) cycling transition at 670.9 nm using the saturated absorption resonance in a Li heat pipe. The remainder of the laser output was sent through an electro-optic modulator, operating at 827 MHz to provide sidebands for hyperfine repumping, and an 80-MHz AOM to provide intensity control and frequency shifting. The laser beam was then expanded to ≈ 2 cm diameter and ≈ 200 mW was available for trapping. The central frequency of the laser at the trapping region was -20 MHz detuned from the cycling transition, or $\Delta \approx 3.4\Gamma$ (natural linewidth, $\Gamma = 5.9$ MHz). The laser beam was split into three roughly equal intensity beams and sent to the trap in the standard retroreflecting configuration with quarterwave plates to achieve the proper polarizations.

Approximately 5×10^6 Li atoms were trapped and cooled to a temperature of about 1 mK with a cloud size of about 1 mm in diameter. Fluorescence from the trapped Li atoms were collected with roughly 1.6% efficiency using a $f/2$ lens inside the chamber and imaged onto a photodiode detector to monitor the MOT intensity. The ionizing electron beam, after passing through the interaction region, was collected by a Faraday cup to monitor the current and minimize backscattering to the interaction region. The ions were extracted by a pulsed electric field (8 V/cm) and, after passing through a drift region, were detected by a two-dimensional position-sensitive detector consisting of three 25-mm-diameter microchannel plates (MCPs) in a Z stack and a resistive anode encoder [31]. The total flight path for an ion produced in the trap to the detector was ≈ 11.5 cm. The typical voltage across the three MCPs was 2250 V with the front MCP floated between -2 kV and -3 kV to vary the ion-impact energy. A grid ring, located ≈ 1 mm in front of the MCPs and floated 100 V more negative, reduced the loss of secondary electrons produced by ion impact on the front MCP. The ion position is determined by magnitudes of the charges collected from the four corners of the specially shaped resistive anode; the charges are converted to voltage pulses by preamplifiers. The ion arrival time is signaled by the fast summed output of the preamplifiers. Ion times of flight were obtained by using electron pulses as the ''start'' and ions striking the detector as the ''stop'' in a time-to-amplitude converter (TAC). The TAC output and pulse-height signals from the four corners of the detector were sent to 11-bit analog-to-digital converters in a CAMAC crate and recorded as event files. The event files were later used to generate TOF spectra as a function of position and pulse height. For each experimental run, we also recorded the total number of ions hitting the detector, the total number of ions arriving within the TAC

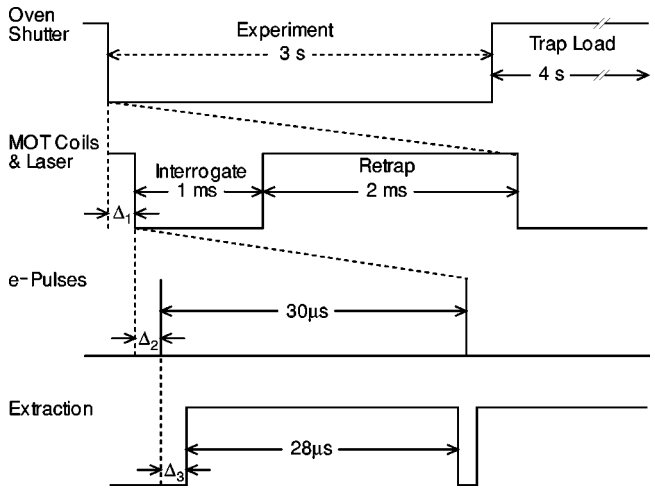

FIG. 2. Schematic of the experimental timing sequence. Three time scales are involved (s, ms, and μs). The first sequence (s) is for trap loading (4 s) and the experimental window (3 s). The second sequence is for interrogation (1 ms) and retrapping (2 ms). $\Delta_1=8$ ms is the delay between the shutter closing trigger and the start of the interrogation period. The third sequence (μs) is for pulsing of the electron beam, extraction field, and the time of flight of the ions. $\Delta_2=50$ μs is the delay between the *B* field off trigger and the first electron pulse. $\Delta_3=260$ ns is the delay between the electron pulse and the extraction field pulse. See text for further details.

window, the electron current in the Faraday cup, and the MOT fluorescence.

During the experiment, the oven shutter, laser light, magnetic field, electron beam, and extraction field were switched with a well-defined time sequence, as shown in Fig. 2. Data were taken only when the oven shutter, laser, and *B* field were turned off, ensuring that the experiment probed only ground-state Li from the trap and that the Li beam from the oven was blocked. The oven shutter was opened for 4 s to load the trap and closed for a 3-s experimental window. This time scale is set by the lifetime of the MOT ($\approx$3 s). During loading, the trapping laser and *B* field were switched on. After closing the shutter, an 8-ms delay (Δ_1) is imposed before the start of the interrogation period in order to allow the shutter to close completely. A single interrogation period lasted for 1 ms, during which time the trapping laser light and *B* field were switched off. This time scale, 1 ms, is set by the time taken for the Li atoms to expand ballistically by 1 mm. During the interrogation period, the electron-beam pulses (100 ns) and ion extraction pulses (28 μs) were switched repetitively with a period of 30 μs, after a delay of 50 μs (Δ_2) to allow the *B* field to decay. The extraction pulses were triggered 280 ns (Δ_3) after the electron-beam pulse. The ion extraction timing left a window of 2 μs for the electron pulse to pass through the interaction region unperturbed by either the *B* field or the ion extraction field. Approximately 30 cycles of electron pulse/ion extraction were delivered during each interrogation period. After each interrogation period, the Li atoms were retrapped by turning on the trapping laser beams and *B* field for 2 ms. Roughly 1000 interrogation/retrap cycles were completed in the 3-s

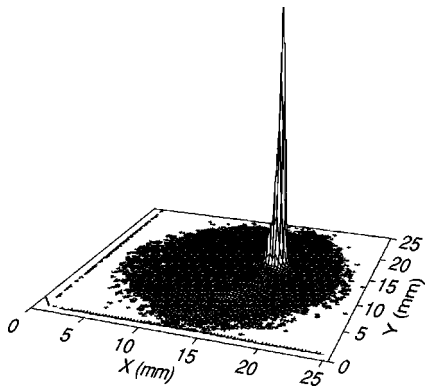

FIG. 3. A contour plot of the ions detected on the position-sensitive detector. The localized spot due to Li^+ from the trapped Li atoms is prominent.

experimental window before the trap required reloading. The entire sequence is repeated many times to build up statistics for the ion ratio measurement. A typical data set requires $\approx$1–2 h at each electron-impact energy. By recording Li^{2+} and Li^+ ions simultaneously in the TOF spectra, there was no need to normalize their relative intensities for variations in the Li target density or electron-beam flux during the long data-acquisition time for the ratio measurement.

III. DATA ANALYSIS

Virtually no Li ions were observed in time-of-flight spectra taken with the *B* field off (no MOT) while other conditions remained the same (electron gun, laser, extraction, and oven shutter being switched as usual). This showed that no appreciable background Li vapor was present in the chamber when the oven shutter was closed and that the measured Li ions came exclusively from the trapped sample. Backgrounds in the TOF spectra were due primarily to H_2 and H_2O residual gases in the chamber. Because Li atoms were confined to a small spot and had small translational momenta, the resulting ions also hit a small area ($\approx$2 mm diameter) of the detector, as shown in Fig. 3. By resorting the event file to include only ions hitting a small area, the background could be reduced by factors of 6–10 for box sizes of 8.5 and 5.8 mm, respectively. A sample TOF spectrum is shown in Fig. 4. The width of the time-of-flight peak for Li^+ was $\approx$160 ns and the flight time $\approx$4.4 μs, for a resolution $\Delta t/t$ of 3.7%.

In order to reduce the multiple-hit probability, the count rate was kept below 5% of the electron gun pulsing frequency at all times. Nevertheless, all TOF spectra were multihit corrected using the following analytic formula [32]:

$$N_A=\frac{N_i}{1-\frac{1}{N}\sum_{j=1}^{i-1}N_j}, \tag{1}$$

where N_A is the true number of counts in the channel i, N is the total number of electron pulses, and N_i is the observed counts in channel i. This correction is required because the TAC is stopped only once (by the first ion arrival) during

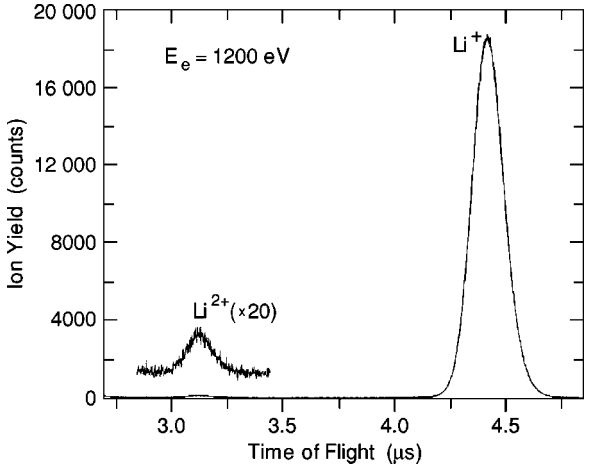

FIG. 4. Ion time-of-flight spectrum recorded at an electron-impact energy of 1200 eV showing Li^{2+} and Li^+.

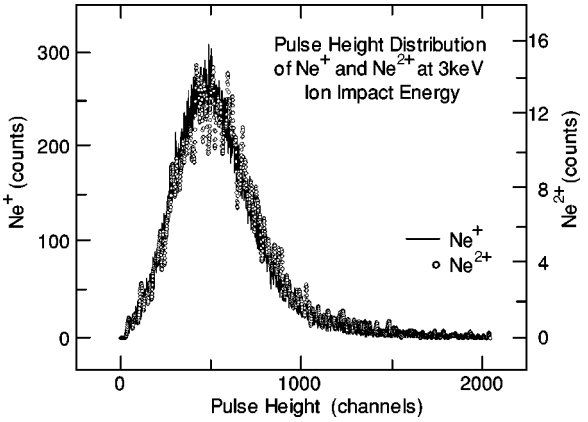

FIG. 5. Pulse-height distributions of Ne^+ and Ne^{2+} ions at the same impact energy of 3 keV, demonstrating that the distributions overlap.

each TOF cycle. Therefore, in cycles where two or more ions were created during one-electron pulse, the fastest ion will be preferentially detected. The multihit-corrected spectra typically yielded ratios $\approx 2\%$ lower than the raw TOF spectra.

The background-subtracted ion yields under the Li^+ and Li^{2+} peaks in the multihit-corrected TOF spectrum were used to calculate the ratio. Typically we acquired at least 2500 counts in the Li^{2+} peak with roughly 1.5 times this number in the background. Four box sizes (2.4, 3, 5.8, and 8.5 mm) were used to obtain the TOF spectra and the charge state ratio in order to study discrimination between different charge states as a function of area. The smallest box size was found to discriminate against detection of Li^{2+} and an average of the ratios obtained using the largest two box sizes is reported here. There were at least three independent runs for every electron energy, which were consistent within statistical errors (typically 3–4 %).

Possible systematic errors in the Li^{2+} to Li^+ ratio can arise from charge-exchange collisions along the ion flight path (≈ 11.5 cm) through the spectrometer. Background pressure was kept at about 2×10^{-9} Torr during the experiment, so charge-changing collisions between outgoing ions and background gas should be negligible. In addition, we tested for charge exchange with other Li atoms in the trap by reducing the number of trapped atoms by somewhat more than a factor of 2. No statistically significant difference in the ratio was observed.

Another systematic error in the Li^{2+} to Li^+ ratio can be caused by different detection efficiencies for Li^{2+} and Li^+ ions. The detection efficiencies for MCP-based detectors depend on the ion-impact energy for ions of the same species. The ratio Li^{2+} to Li^+ was measured for ion-impact energies ranging from 1 keV to 3 keV, by varying the floating voltage on the front MCP. It was found that the measured ratios agreed within statistical errors for floating voltages equal to or greater than -2 kV. However, this does not necessarily imply that the charge states are detected with equal efficiencies, since the pulse-height distribution for the singly and doubly charged ions can differ. If the pulse-height distributions of the two charge states are the same, then it is assumed that the detection efficiencies will be the same. In order for the pulse-height distributions to be the same, the ion impact energy needs to be the same; i.e., 2-kV Li^{2+} should give the same pulse-height distribution as 4-kV Li^+. It is impractical to measure this small correction to the observed ratio at a given floating voltage using Li TOF spectra, because the Li^{2+} to Li^+ ratio is very low ($\leqslant 0.4\%$) and perfect normalization of Li trap density and electron-beam flux between long runs would be necessary. Therefore, to evaluate the efficiency correction factor, we measured the 2+ to 1+ ratio for both He and Ne, where a constant target thickness was easily maintained using a flow controller to admit the sample gases to the entire turbo-pumped chamber. The chamber pressures were 1×10^{-6} and 5.6×10^{-7} Torr for He and Ne, respectively. Otherwise, the measurements were done under the same conditions as the experiment on Li; i.e., with electron gun, extraction field, *B* field, and oven shutter, all being switched. Ratios were then obtained by two methods: (1) using 1+ and 2+ ion yields from the same TOF spectrum with a floating voltage of -2.0 kV, and (2) using the ion yields of 1+ and 2+ from spectra with different floating voltages (-1.5 kV and -3 kV) such that the 1+ and 2+ ions have the same impact energy. The pulse-height distributions of the 1+ and 2+ ions do indeed overlap when accelerated to the same impact energy, as shown for Ne in Fig. 5. It was found that the ratios measured using method (2) were consistently lower than those measured using method (1), as one would expect, because for any fixed floating voltage the 2+ ions will have a pulse-height distribution shifted to higher values and therefore will be preferentially detected. The 2+ to 1+ ratios that we measured for He were in good agreement with those reported in the literature [17,18]. The difference between the two methods, i.e., the correction factor, was 3% for He and 7% for Ne. It was observed in previous studies using a double MCP detector [33] that the saturation of the MCP detection efficiency depends on the mass of the ions. The detection efficiency of lighter ions saturates faster as a function of impact energy than that of heavier ions, as we observe here. Thus, the correction for our Li measurement should fall between those of He and Ne. We have applied a correction factor of 5% and report on the Li^{2+}

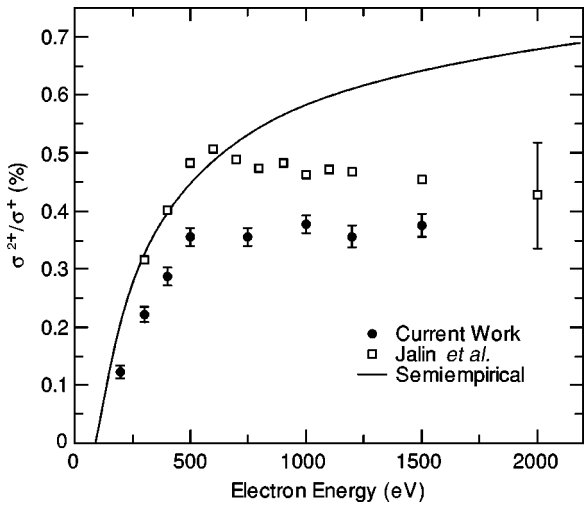

FIG. 6. The Li^{2+} to Li^{+} ratio as a function of electron energy. Closed circles are current work. Open squares are ratios of the absolute cross-section measurements by Jalin *et al.* [28]. Solid curve shows ratios obtained from semiempirical formulations for single [34] and double ionization [19].

to Li^{+} ratios as 95% of the raw values we obtained using floating voltages of -2 kV or higher.

IV. RESULTS AND DISCUSSION

Our measurements of the Li^{2+} to Li^{+} production cross-section ratios for electron-impact energies ranging from 200 eV to 1500 eV are shown in Fig. 6 and in Table I. Our reported error bars for the ratio (about 5%) are due to statistics and consistency between runs. We did not add an additional uncertainty for the detection-efficiency correction factor. The ratio rises as a function of electron-impact energy, and seems to reach a plateau at 500 eV where it remains at about 0.37% up to the maximum energy of 1500 eV. To our knowledge, the only other measurement on double ionization of Li by electron impact is that of Jalin *et al.* [28]. In that measurement, absolute single- and double-ionization cross sections were measured separately using different detectors. The ratios of their measured absolute cross sections are also shown in Fig. 6. The uncertainty of each of their absolute measurements was -15% and $+20\%$. We estimate a $\pm 20\%$ error bar for their ratios. For clarity, this error bar is only placed on one of the data points in Fig. 6. It can be seen clearly that our measurements are systematically lower, but show energy dependence similar to that observed by Jalin *et al.* Most of their ratios overlap with the present results within the spread of the combined error bars.

TABLE I. Measured Li^{2+} to Li^{+} ratio.

E_e (eV)	Ratio (%)
200	0.123(12)
300	0.222(13)
400	0.288(15)
500	0.356(15)
750	0.355(15)
1000	0.377(15)
1200	0.356(19)
1500	0.375(19)

To date, there is no *ab initio* calculation for double ionization of Li by electron impact. Therefore, we compare the measurements to semiempirical formulations. These formulations assume that all electrons of an atom contribute to the total ionization cross section, and that the contributions from all electrons within a given subshell are identical. The single-ionization cross sections were obtained by using the semiempirical formula of Lotz [34]:

$$\sigma=\sum_{i=1}^{N} a_i q_i \frac{\ln(E/P_i)}{EP_i}\{1-b_i\exp[-c_i(E/P_i-1)]\},$$
$$E\geqslant P_i, \tag{2}$$

where E is the electron-impact energy; P_i is the binding energy for electrons in the ith subshell; q_i is the number of equivalent electrons in the ith subshell; a_i, b_i, and c_i are individual constants. We have used the constants given by Lotz $[P(2s)=5.39$ eV, $P(1s)=58$ eV, $a=4.0, b=0.70, c=2.4]$ to calculate the values of the single-ionization cross sections. The double-ionization cross sections were obtained using the similar, recent semiempirical formulation of Bélenger *et al.* [19],

$$\sigma_n=\frac{a(n)N^{b(n)}}{(I_n/\mathrm{Ry})^2}\left(\frac{u}{u+1}\right)\frac{\ln(u+1)}{u+1}[10^{-18}\mathrm{cm}^2], \tag{3}$$

where $u=E/I_n-1$, E is the incident electron energy; I_n is the minimal ionization energy required to remove n outermost electrons from the target; N is the total number of target electrons; $a(n)$ and $b(n)$ are constants; and 1 Ry = 13.6 eV. [From that paper, for $n=2, a(n)=14$ and $b(n)=1.08$.] The ratio of these two cross sections as a function of electron energy is plotted in Fig 6. This ''semiempirical'' ratio is larger than our measurement throughout the entire energy range measured, and does not show the plateaulike structure above 500 eV. If instead of the the Lotz formula we use the *ab initio* single-ionization cross sections calculated by Bray [21] (which agree well with the measurements by Jalin *et al.*) then the resulting ratio for Li^{2+} to Li^{+} is yet higher and in even poorer agreement with our measurements. It should be noted that the Bélenger *et al.* semiempirical formula predicts larger double-ionization cross sections for metallic atoms (Fe, Cu, Ag, and Bi) than experimentally observed [19]. This might also be the case for Li, and thereby cause the Li^{2+} to Li^{+} semiempirical ratios to be larger than observed experimentally.

It is also of interest to compare our plateau value (0.37%) for the ratio of double-to-single ionization by electron impact to that predicted for the shake-off mechanism. In a previous study of the ratio of double-to-single ionization of lithium by fast heavy-ion impact [35], the authors calculate the probability to shake off an electron after removal of a $1s$ or $2s$ electron by the ionizing projectile. For an initially created $1s$ hole state, the probability to shake off a $1s(2s)$ electron was

calculated to be 0.38% (0.38%). For an initially created $2s$ hole, the probability to shake off a $1s$ electron was calculated to be 0.03%. In order to use these shake-off values to predict the high-energy limit of the ratio by electron-impact ionization, knowledge of the partial cross sections for $1s$ and $2s$ ionizations is required. One can obtain the partial cross sections for $1s$ and $2s$ electron-impact ionization either from *ab initio* theory [25] or by using the relationship between the photoabsorption cross section $S(-1)$ sum rule [36] and the charged particle impact ionization cross sections [37]. Asymptotically, the Bethe formula for the ionization cross section as a function of projectile energy can be written as follows:

$$\sigma_i E/R = (4\pi a_0^2) M_i^2 \ln(4Ec_i/R), \tag{4}$$

where σ_i is the total ionization cross section, E is the incident projectile energy, c_i is a constant that depends on the properties of the target, and R and a_0 are the Rydberg (energy unit) and Bohr radius, respectively. Ratios of ionization cross sections in the high-energy limit are therefore determined roughly by the leading factor M_i^2, the squared dipole moment, which corresponds to the portion of $S(-1)$ leading to ionization, $S_i(-1)$, i.e.,

$$M_i^2 = S_i(-1) = \int_{IP}^{\infty} (1/E)(df/dE)dE, \tag{5}$$

where E is the energy and f is the oscillator strength. The M_i^2 for $2s$ ionization will be given roughly by the $S_i(-1)$ integral between the $2s$ and $1s$ ionization thresholds, 5.39 and 65.0 eV, respectively. The M_i^2 for $1s$ ionization will be given by the $S_i(-1)$ integral above 65 eV. These spectral sums for lithium are conveniently given in Berkowitz's recent book [36]. Using Table 2.6 of that book, we find that the $S_i(-1)$ sum for $2s$ ionization is 0.233, and that for $1s$ ionization is 0.195, for an asymptotic ratio $\sigma_{2s}/\sigma_{1s} = 1.2$. (The coefficients of the Bethe logarithm term in Younger's expressions for the $1s$ and $2s$ partial cross sections yield a similar value for the ratio, $\sigma_{2s}/\sigma_{1s} = 1.04$.) Using the ratio obtained from photoabsorption data, $\sigma_{2s}/\sigma_{1s} = 1.2$, we obtain a shake-off probability of 0.36%. This asymptotic value is surprisingly near the plateau value that we observe (0.37%).

Finally, we compare to ionization by other projectiles, heavy ions, and photons. We note that our plateau value for the electron-impact double-to-single ionization ratio agrees with the observed $2+$ to $1+$ ratio of $(0.34 \pm 0.07)\%$ induced by fast heavy-ion impact (95 MeV/amu N^{7+}) [35]. In that work, the authors calculate an asymptotic $2+$ to $1+$ ratio of 0.29%, of which 25% of the $2+$ yield is due to shake off and the remaining $2+$ yield is due to TS-2 processes. (The TS-2 process was defined as a two-step process, involving *two* interactions between the projectile and the target electrons.) The asymptotic ratio for photon impact is calculated to be a factor of ≈ 10 higher [38]. In general, the asymptotic $2+$ to $1+$ ratio for photon impact is expected to be larger, since in charged particle ionization the energy transfer is not fixed and lower energy transfers favor single ionization.

V. CONCLUSION

In summary, the Li^{2+} to Li^{+} production cross-section ratio by electron impact was measured for electron energies ranging from 200 eV to 1500 eV. The measured ratios range from ≈ 0.1 to 0.4 % and appear to reach a plateau value of 0.37% above 500 eV. The $2+$ to $1+$ ratios were found to be systematically lower than those of Jalin *et al.* and those predicted by semiempirical formulas. The trapped atom sample combined with an ion imaging time-of-flight spectrometer offers some advantages for these measurements: (1) elimination of dimers and impurities, (2) enhanced control of ion collection efficiency, and (3) reduction of background through position-sensitive cuts on the data. Through careful assessment of systematics, the accuracy achieved ($\approx 5\%$) is a significant improvement over the single earlier measurement. We hope that this result will motivate theorists to perform *ab initio* calculations for this relatively simple system and act as a benchmark for those studies.

ACKNOWLEDGMENTS

We thank M. Lindsay for assistance in the early stages of this work, R. Ali for advice in developing the event mode software, and M. Inokuti for helpful discussions. This work was supported by the Chemical Sciences, Geosciences, and Biosciences Division of the Office of Basic Energy Sciences, Office of Science, U.S. Department of Energy, under Contract No.W-31-109-Eng-38.

[1] T. D. Märk and G. H. Dunn, *Electron Impact Ionization* (Springer, Vienna, 1985), and references therein.
[2] I. Bray and A.T. Stelbovics, Phys. Rev. Lett. **70**, 746 (1993).
[3] D. Kato and S. Watanabe, Phys. Rev. Lett. **74**, 2443 (1995).
[4] K. Bartschat and I. Bray, J. Phys. B **29**, L577 (1996).
[5] M.S. Pindzola and F. Robicheaux, Phys. Rev. A **54**, 2142 (1996).
[6] T.N. Rescigno, M. Baertschy, W.A. Issacs, and C.W. McCurdy, Science **24**, 2474 (1999).
[7] M.B. Shah, D.S. Elliott, and H.B. Gilbody, J. Phys. B **20**, 3501 (1987).
[8] See, for example, I. Bray, Can. J. Phys. **74**, 875 (1996).
[9] P. Lamy, B. Joulakian, C.Dal. Cappello, and A. Lahmam-Bennani, J. Phys. B **29**, 2315 (1996).
[10] A. Kheifets, I. Bray, A. Lahmam-Bennani, A. Duguet, and I. Taouil, J. Phys. B **32**, 5047 (1999).
[11] J. Berakdar, Phys. Rev. Lett. **85**, 4036 (2000).
[12] M.S. Pindzola, D. Mitnik, and F. Robicheaux, Phys. Rev. A **59**, 4390 (1999).
[13] B. El Marji, A. Duguet, A. Lahmam-Bennani, M. Lecas, and H.F. Wellenstein, J. Phys. B **28**, L733 (1995).
[14] I. Taouil, A. Lahmam-Bennani, A. Duguet, and L. Avaldi, Phys. Rev. Lett. **81**, 4600 (1998).
[15] A. Lahmam-Bennani, I. Taouil, A. Duguet, M. Lecas, L. Avaldi, and J. Berakdar, Phys. Rev. A **59**, 3548 (1999).
[16] A. Dorn, A. Kheifets, C.D. Schröter, B. Najjari, C. Höhr, R.

Moshammer, and J. Ullrich, Phys. Rev. Lett. **86**, 3755 (2001).
[17] P. Nagy, A. Skutlartz, and V. Schmidt, J. Phys. B **13**, 1249 (1980).
[18] M.B. Shah, D.S. Elliott, P. McCallion, and H.B. Gilbody, J. Phys. B **21**, 2751 (1988).
[19] C. Bélenger, P. Defrance, E. Salzborn, V.P. Shevelko, H. Tawara, and D.B. Uskov, J. Phys. B **30**, 2667 (1997).
[20] H. Deutsch, K. Becker, and T.D. Mark, J. Phys. B **29**, L497 (1996).
[21] I. Bray, J. Phys. B **28**, L247 (1995).
[22] J. Colgan, M.S. Pindzola, D.M. Mitnik, D.C. Griffin, and I. Bray, Phys. Rev. Lett. **87**, 213201 (2001).
[23] D.W. Chang and P.L. Altick, J. Phys. B **28**, 1049 (1995).
[24] X.Z. Qian and S.F. Pan, Phys. Lett. A **211**, 281 (1996).
[25] S.M. Younger, J. Res. Natl. Bur. Stand. **87**, 49 (1982).
[26] R.H. McFarland and J.D. Kinney, Phys. Rev. **137**, A1058 (1965).
[27] I.P. Zapesochnyi and I.S. Aleksakhin, Zh. Éksp. Teor. Fiz. **55**, 76 (1968) [JETP **28**, 41 (1969)].
[28] R. Jalin, R. Hagemann, and R. Botter, J. Chem. Phys. **59**, 952 (1973).
[29] R.S. Schappe, T. Walker, L.W. Anderson, and Chun C. Lin, Phys. Rev. Lett. **76**, 4328 (1996).
[30] R. Dörner, V. Mergel, O. Jagutzki, L. Spielberger, J. Ullrich, R. Moshammer, and H. Schmidt-Böcking, Phys. Rep. **330**, 95 (2000).
[31] Quantar Technology Inc., Santa Cruz, CA.
[32] D. V. O'Connor and D. Phillips, *Time Correlated Single Photon Counting* (Academic, London, 1984).
[33] H.C. Straub, M.A. Mangan, B.G. Lindsay, K.A. Smith, and R.F. Stebbings, Rev. Sci. Instrum. **70**, 4238 (1999).
[34] W. Lotz, Z. Phys. **216**, 241 (1968); **206**, 205 (1967).
[35] B. Skogvall, J.Y. Chesnel, F. Fremont, D. Lecler, X. Husson, A. Lepoutre, D. Hennecart, J.P. Grandin, B. Sulik, A. Salin, and N. Stolterfoht, Phys. Rev. A **51**, R4321 (1995).
[36] J. Berkowitz, *Atomic and Molecular Photoabsorption* (Academic Press, San Diego, 2002).
[37] M. Inokuti, Rev. Mod. Phys. **43**, 297 (1971).
[38] H.W. van der Hart and C.H. Greene, Phys. Rev. Lett. **81**, 4333 (1998).